PHYSICAL REVIEW B **81**, 085322 (2010)

Scanning microscopy of nuclear spin polarization via quantum Hall edge channels

T. Nakajima,* Y. Kobayashi, S. Komiyama, and M. Tsuboi
Department of Basic Science, University of Tokyo, 3-8-1 Komaba, Meguro-ku, Tokyo 153-8902, Japan

T. Machida
Institute of Industrial Science, University of Tokyo, 4-6-1 Komaba, Meguro-ku, Tokyo 153-8505, Japan
(Received 5 October 2009; published 17 February 2010)

Nuclear spin polarization is probed via hyperfine interaction with spin-split edge channels. By scanning the edge channels with a biased metal side gate, the local profile of nuclear spin polarization is imaged with a resolution of ~14 nm, determined by the extension of the edge-state wave function. Distribution of the nuclear spins dynamically polarized by the edge channels is found to be localized in a region as narrow as 35 nm at the lowest current (0.1 nA) but broadens with increasing current. The decay process is studied in detail with the same technique and the temporal dynamics of the nuclear polarization are interpreted in terms of the interplay of diffusion, electron-nuclear spin interaction, and spin-lattice relaxation.

DOI: 10.1103/PhysRevB.81.085322 PACS number(s): 73.43.Fj, 76.60.−k, 72.25.−b

I. INTRODUCTION

Spin degrees of freedom of electrons and nuclei in semiconductor nanostructures are promising candidates for scalable qubits in solid-state devices. Recent experiments have successfully achieved coherent control of electronic spin states in quantum dots.[1,2] However, the dephasing time is limited to be $T_2^* \sim 10$ ns because of the slow fluctuations of the effective magnetic field induced by the hyperfine interaction with the surrounding nuclear spins in GaAs crystals.[1–5] The coherence time can be prolonged to $T_2 \sim 1$ μs by the spin-echo technique[1,6] but still suffers from the nuclear-nuclear spin-interaction mediated by virtual flip-flop interactions with electron spins.[7–9] Even on a much longer time scale of ~100 s, the electron-nuclear spin interaction manifests itself and causes oscillatory leakage current in the spin-blockade regime.[10] These drawbacks are inevitable as long as GaAs host crystals are used for the benefit of their outstanding electronic properties.

When multiple spin qubits are integrated on a single device, an additional complication may arise from nuclear spin diffusion. Since the total nuclear spin angular momentum has an extremely long lifetime, polarized nuclear spins diffuse through dipole-dipole interactions, leading to interference with neighboring circuitry. The unwanted polarization brings about serious degradation in device performance, long-term stability and reproducibility. While nuclear spin is such a significant obstacle from the viewpoint of the electron spin manipulation, there are also proposals to utilize it as a spin memory[11] or another implementation of qubit.[12] Therefore, thorough understanding of the nuclear spin dynamics in nanostructure devices is highly desirable both for positive application and proper elimination of the nuclear spin polarization.

In this work, we investigate the dynamics of nuclear spin polarization and relaxation in a nanometer scale region. Nuclear spin polarization is pumped and detected locally via spin-resolved edge channels in the integer quantum Hall regime.[13–15] Although the pumped nuclear polarization is supposed to be localized in the vicinity of the edge channels, its true spatial profile has been completely unknown because of the lack of experimental studies. The technique of scanning edge channels reported here directly visualizes the profile of nuclear spin polarization as well as its dynamics. We first describe the measurement scheme in Sec. II. In Sec. III, profiles of pumped nuclear polarization are displayed. The profiles are shown to depend on the polarity and the amplitude of bias currents, reflecting the self-consistent reconstruction of electronic structure of the edge channels. The decay process of localized polarization is studied in Sec. IV, where diffusion is suggested to play an essential role, in addition to electron-nuclear spin interaction and spin-lattice relaxation.

II. EXPERIMENTAL METHODS

Devices were fabricated in two different modulation-doped GaAs/AlGaAs heterostructure crystals, A and B. The density and the mobility of the two-dimensional electron gas (2DEG) at 4.2 K are, respectively, 3.0×10^{15} m^{-2} and 30 m^2/V s in crystal A and are 2.0×10^{15} m^{-2} and 90 m^2/V s in crystal B. Similar experimental results have been seen in both crystals but we present below only the results obtained in crystal B for reason of space. The measurements were performed at $T=30$ mK. The magnetic field was chosen to be $B\approx4.2$ T, corresponding to the integer quantum Hall plateau of the filling factor of $\nu=2$. The profile of dynamic nuclear polarization (DNP) via interedge-channel scattering was found to change slightly after different cooling cycles, probably because the profile is sensitive to the *ad hoc* configuration of impurity scatterers. Reproducibility was obtained, however, by slightly adjusting the magnetic field (within ±0.1 T).

The device geometry is schematically shown in Fig. 1(a). Two front cross gates (CGs) are prepared at a distance of 20 μm and a front side gate is deposited along the mesa edge bounded by the two CGs. When the CGs are negatively biased so that the filling factor underneath the CGs is $\nu_G=1$, the electrochemical potentials of the source and the drain

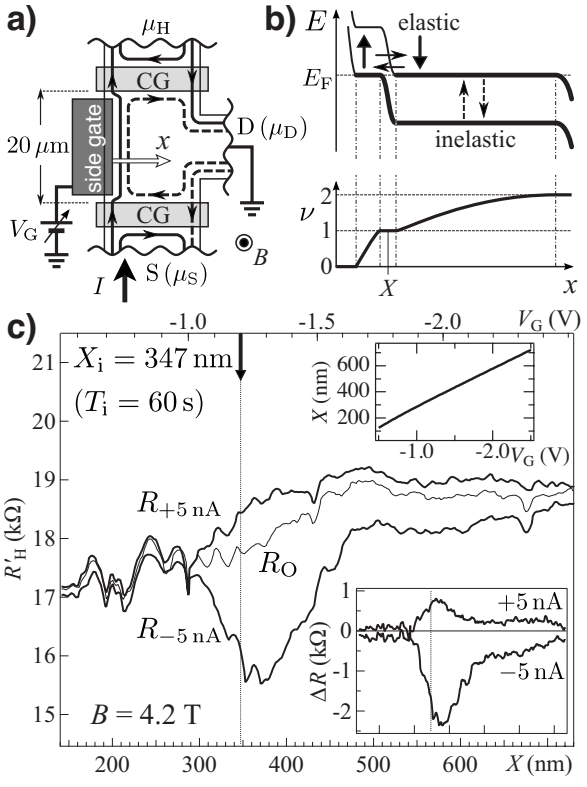

FIG. 1. (a) Schematic of sample configuration. The outer (inner) edge channel carries spin-up (down) electrons. The spin-split edge channels are unequally populated ($\mu_\uparrow \neq \mu_\downarrow$) along the side gate, where the location of the edge channels is scanned by the bias voltage V_G applied to the side gate. (b) Energy-level diagram (upper panel) and the local filling factor ν of the edge states. (c) Differential Hall resistance at B=4.2 T as a function of X derived from V_G (upper right inset). The curves R_O and $R_{\pm 5\ nA}$ are taken with the pumping currents of I_i=0 and ±5 nA, respectively, for T_i=60 s. The vertical dotted line marked by an arrow indicates the position $X=X_i$ of pumping. The lower right inset shows the resistance changes, $\Delta R=R_{\pm 5\ nA}-R_O$, indicating the profile of nuclear polarization.

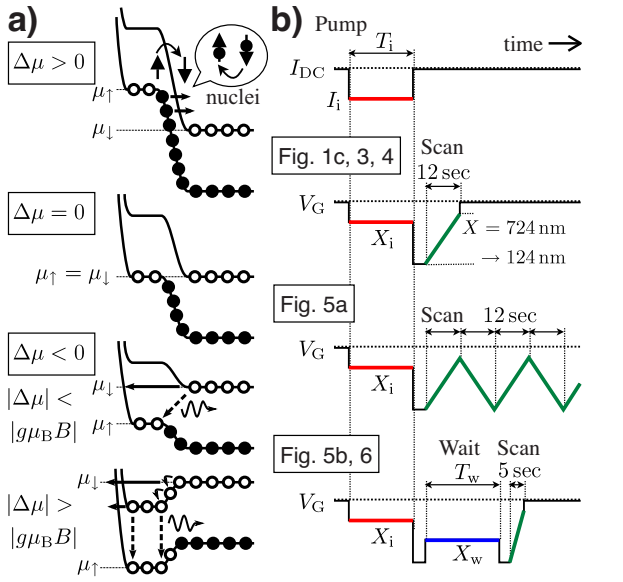

FIG. 2. (Color online) (a) Structure of the edge channels for negative $I_i<0$ ($\Delta\mu>0$) and positive $I_i>0$ ($\Delta\mu<0$) pump currents. Filled (open) circles denote completely (partially) filled electron states. (b) Time sequences of the gate voltage V_G in respective measurements (lower three panels) along with the pump current I_i (top panel). Differential Hall resistance R'_H is studied during the scans of V_G.

contacts populate the up-spin (↑) outer edge channel and the down-spin (↓) inner edge channel up to $\mu_\uparrow=\mu_S$ and $\mu_\downarrow=\mu_D$, respectively, at the corner of the lower CG. The unequal population is controlled by the source-drain current I such that $\Delta\mu=\mu_S-\mu_D=-(h/e)I$ with unit charge e, where the polarity of current I is defined to be positive ($I>0$) when a positive charge flows from the source to the drain contact ($\Delta\mu<0$). The unequally populated edge channels extend along the edge defined by the side gate for a length of ℓ_{edge}=20 μm.

It has been shown in earlier experiments[13–16] that spin-flip scattering between unequally populated spin-resolved edge channels induces nuclear polarization along the edge channels through the simultaneous flip-flop process and the nuclear polarization in turn causes the scattering rate to change [see Fig. 2(a)]. Despite these extensive studies in the past, the local profile of the spatial distribution of the generated nuclear polarization has been unknown. In this work we utilize the side gate to scan the edge channels sideways toward interior/exterior regions of the mesa structure. The bias voltage V_G applied to the side gate controls the position of the edge channels, which enables us to define independently the location of pumping and the location of probing.

Contact hyperfine interaction between a nuclear spin **I** of GaAs nuclei and an electron spin **S** of conduction electrons in edge channels,

$$H_{\text{hyperfine}} = A\mathbf{I}\cdot\mathbf{S} = \frac{A}{2}(I^+S^- + I^-S^+) + AI_zS_z, \qquad (1)$$

is the relevant mechanism both for pumping and probing nuclear polarization, where $A(>0)$ is the hyperfine constant. When the dc source-drain current is negative, $I<0$ ($\Delta\mu>0$), electron spin-flip scattering from up to down takes place as illustrated in Fig. 2(a), resulting in nuclear spin-flop scattering from down to up through the term $\frac{A}{2}(I^+S^-+I^-S^+)$ in Eq. (1). The negative current thus leads to DNP in the up polarity ($\langle I_z\rangle>0$). Throughout this paper, we refer to this polarity as "negative" polarization. Through the term AI_zS_z in Eq. (1), the average nuclear polarization $\langle I_z\rangle$ is equivalent to the generation of the local effective magnetic field of $\Delta B = A\langle I_z\rangle/(g\mu_B)$, where $g=-0.44$ is the electronic g factor in GaAs. Since $g<0$, negative nuclear polarization ($\langle I_z\rangle>0$) is equivalent to a negative magnetic field, which leads to the reduction in effective Zeeman energy. This increases the rate of scattering due to spin-orbit interaction,[17] which is experimentally detected as a decrease in the Hall resistance. Conversely, positive current $I>0$ ($\Delta\mu<0$) generates positive nuclear polarization ($\langle I_z\rangle<0$) as illustrated in the lower two panels of Fig. 2(a), which increases the Hall resistance. In the present experiments, the Hall resistance is studied via three-terminal resistance $R_H=-(\mu_H-\mu_D)/(eI)$ [Fig. 1(a)]. It

would be h/e^2 in the absence of interedge scattering and $h/(2e^2)$ in the case of complete equilibration in the configuration shown in Fig. 1(a).[18–20]

To describe experimental results, we define the location of the edge channels, $x=X$, as that of the incompressible stripe with respect to the edge of the side gate ($x=0$) (Fig. 1(b)). Given the voltage V_G of the side gate 100 nm above the 2DEG, the electron density is derived as a function of x in a theoretical model considering electrostatics.[21] Here we assume that the influence of the shallowly etched mesa edge is negligible because it is far from the potential wall created by the side gate. The incompressible stripe is then found to be at the position $X(V_G)$ where the electron density is half the bulk value and the local filling factor is $\nu_{loc}=1$. The curve of X versus V_G obtained for the present device is displayed in the upper inset of Fig. 1(c), showing that control of X over 100 nm through 700 nm with a nanometer scale resolution is possible.

III. NANOSCALE PROFILE OF DNP

As illustrated in the top panel of Fig. 2(b), nuclear polarization is pumped by applying a dc current $I=I_i$ for an interval of T_i with the edge channels fixed at a location of $X(V_G)=X_i$. After the pumping current is turned off at $t=T_i$, the edge channels are scanned by V_G as illustrated in the second panel from the top in Fig. 2(b). The profile of the pumped polarization is studied by measuring the differential Hall resistance, $R'_H=-\partial(\mu_H-\mu_D)/e\,\partial I$, as a function of $X(V_G)$, with an ac of 1 nA at 508 Hz. The rate of V_G scans is $dV_G/dt=0.167$ V/s ($dX/dt\sim 50$ nm/s) so that one scan takes 12 s.

Three curves of R'_H versus V_G displayed in Fig. 1(c) are taken after the pumping for $T_i=60$ s at $X_i=347$ nm in three different conditions of $I_i=0$ and ± 5 nA, where X values on the horizontal scale is derived from V_G. The Hall resistance R_O taken without pumping ($I_i=0$) for reference shows irregular structures. We have confirmed in additional experiments that identical structures are reproduced in different scans of V_G. The structures are hence concluded to be "fingerprints" ascribed to the edge-specific distribution of local scatterers.[22] The curves marked as $R_{+5\ nA}$ and $R_{-5\ nA}$ are taken, respectively, with $I_i=+5$ and -5 nA. They indicate that R'_H increases (decreases) from R_O with $I_i>0$ ($I_i<0$) as expected. Shown in the lower inset of Fig. 1(c) are the curves of the difference, $\Delta R(X)=R'_H(X)-R_O(X)$, which is identified as the profile of the spatial distribution of nuclear polarization. In the following, we display and discuss only the difference $\Delta R(X)$ and refer to it as the profile of nuclear spin polarization. Unless otherwise stated, all the data of $\Delta R(X)$ shown below are obtained by repeating the procedure described in the above ten times and averaging the results, where each procedure is performed after waiting for 30 min: the waiting time was chosen to certify thermal equilibration of the nuclear spin system.

Figure 3(a) displays the profiles of the nuclear polarization obtained by pumping at $X_i=464$ nm for $T_i=60$ s with different pumping currents I_i. The polarization increases its amplitude with increasing $|I_i|$ from 0.1 to 18 nA. Though not

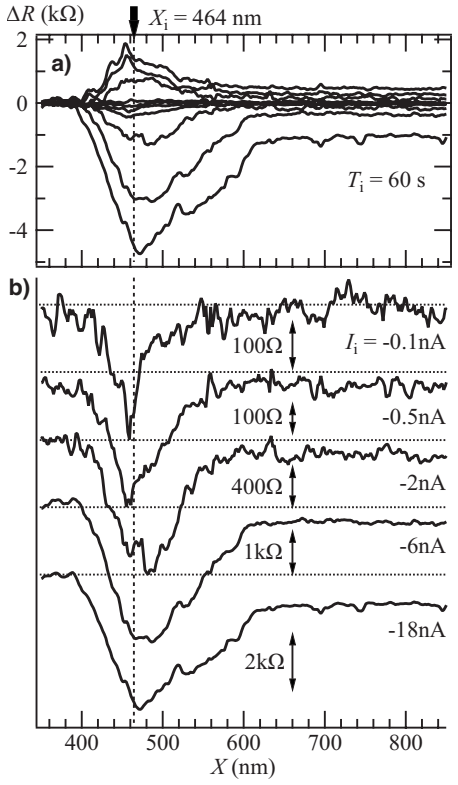

FIG. 3. (a) Profiles of the nuclear spin polarization obtained with $I_i=\pm 0.1$, 0.5, 2.0, 6.0, and 18 nA at $X_i=464$ nm for $T_i=60$ s. The position X is scanned from 850 to 350 nm by varying V_G from -3.0 to -1.2 V. The curves are obtained by repeating the measurement procedure [Fig. 2(b)] more than once and averaging the results. The number of the repeated measurements is 25 for the curves of $I_i=\pm 0.1$ and 0.5 nA, 15 for those of $I_i=\pm 2.0$ nA, and 10 for $I_i=\pm 6.0$ and 18 nA. (b) Closeup of the profiles for $I_i<0$, shown with a normalized peak height. Each curve is offset for clarity with each zero indicated by a horizontal dotted line. The narrowest profile for $I_i=-0.1$ nA suggests that the resolution of measurement is as small as ~ 14 nm.

clear in Fig. 3(a), Fig. 3(b) shows that the distribution is as narrow as 35 nm with the smallest current, $I_i=-0.1$ nA ($\Delta\mu>0$), but is broadened around $X\approx X_i$ with increasing $|I_i|$. In addition, a backgroundlike component is noted to show up in a deeper region of $X>600$ nm for $|I_i|>2$ nA.

Most simply considered, quasielastic flip-flop interedge scattering via hyperfine interaction is expected to take place only in the vicinity of an incompressible stripe ($\nu=1$) as illustrated in Fig. 1(b) and in the top panel of Fig. 2(a). Resultant polarization is hence distributed over the extension of the electron wave function in the edge channels, which is given by the magnetic length $\ell_B=13$ nm. Noting that the width of the $\nu=1$ incompressible stripe is narrow (~ 1 nm),[23] we expect that polarization develops in a narrow range of ~ 14 nm. In the present experiment, the polarization is probed with the microscopy in which finite resolution is given by the same extension of the edge channels (~ 14 nm). Since an experimentally obtained image is determined by the convolution of the profile of polarization and the resolution of microscopy, the image is expected to be broadened to ~ 28 nm, which is in substantial agreement

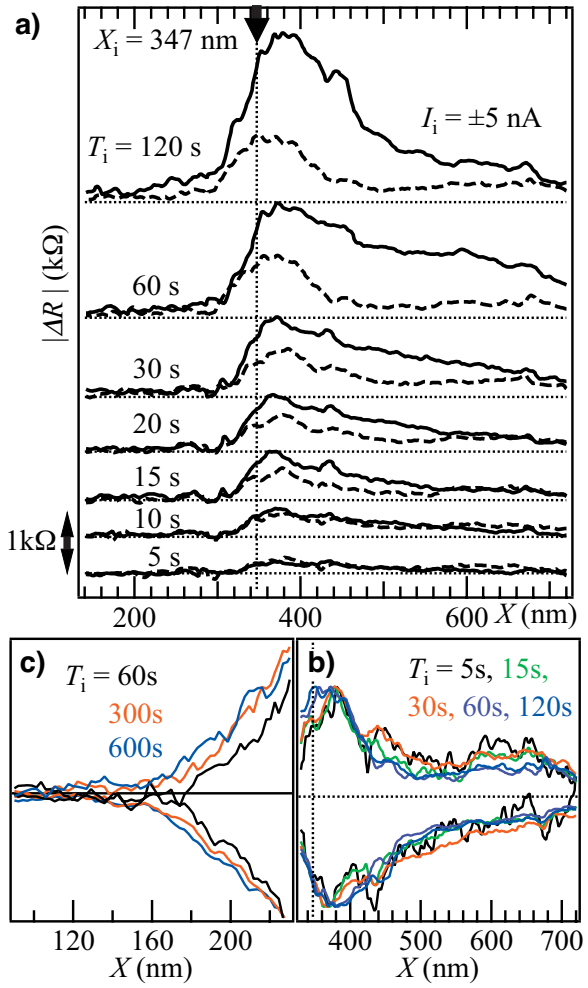

FIG. 4. (Color) (a) Growth of nuclear polarization with $I_i = -5$ nA (solid lines) and $I_i = +5$ nA (dashed lines) at $X_i = 347$ nm. (b) Profiles of nuclear polarization for $T_i = 5$ s (black), 15 s (green), 30 s (red), 60 s (purple), and 120 s (blue) are replotted with a normalized peak height, showing that the shape of the profile is substantially unchanged during the growth of polarization. (c) Closeup of the edge region ($X < X_i$) of the similarly normalized profiles for $T_i = 60$ s (black), 300 s (red), and 600 s (blue).

with the observation (35 nm) in the limit of low current.[24] We thus conclude that the nuclear polarization is pumped and probed in the vicinity of the incompressible stripe of $\nu = 1$.

Let us consider broader distribution found at higher values of $|I_i|$. Simple interpretation in terms of lateral diffusion of nuclear spin polarization is not likely. This is because such diffusion would equally affect the sharp distribution obtained with the lowest current ($I_i = -0.1$ nA). Figure 4(a) shows dependence of the profile on the pumping time T_i for $I_i = -5$ nA (solid lines) and $I_i = +5$ nA (dashed lines). The profile is found to be substantially unchanged for $T_i = 5$ up to 120 s while the magnitude of the polarization increases with time: This is evident in Fig. 4(b), where the profiles of $T_i = 5$, 15, 30, 60, and 120 s are displayed with a normalized amplitude for comparison. It is hence indicated that the broader distribution originates substantially from the distributed profile of flip-flop scattering *in situ*, rather than lateral diffusion. [Nevertheless, the influence of diffusion is discernible in Fig. 4(c) as will be discussed later.]

We will suggest below the relevance of the self-consistent reconstruction of edge-channel profile at larger values of $\Delta\mu$ as well as an elevated local electron temperature. When $\Delta\mu$ is finite, excess charges are accumulated in the edge channels and the edge configuration is thereby reconstructed because the electrostatic potential is deformed self-consistently:[25–27] for $\Delta\mu > 0$ ($I_i < 0$), the width of the $\nu = 1$ incompressible stripe increases with increasing $\Delta\mu$, leading to flip-flop scattering in a wider region [the top panel in Fig. 2(a)]. For $\Delta\mu < 0$ ($I_i > 0$), flip-flop scattering occurs not only in the incompressible region but also in the $0 < \nu < 1$ compressible region as illustrated in the lower two panels of Fig. 2(a). In both polarities of current, therefore, the broadening of the profile around $X \approx X_i$ is accounted for by the edge-channel reconstruction.

In addition to the broadening around X_i, backgroundlike distribution shows up in a region deeper away from X_i, say $X > X_i + 100$ nm. We note that $\Delta\mu$ reaches a value ($|\Delta\mu| = 52$ μeV for $I_i = \pm 2$ nA, for instance) comparable with the spin-splitting energy ($|g\mu_B B| = 107$ μeV). Interedge scattering in the energy window of $\Delta\mu$ (~ 0.6 K) may result in a significant rise in the local electron temperature T_e in the edge channels. When T_e is elevated in the compressible region of $1 < \nu < 2$, inelastic electron scattering accompanied by simultaneous emission/absorption of phonons is possible as shown in Fig. 1(b). We hence suppose that the polarization in a region of $X > X_i + 100$ nm is caused by the phonon-assisted (inelastic) flip-flop processes[28,29] in the compressible region.

Returning to Figs. 1(c), 3(a), and 4(a), we note that the amplitude of nuclear polarization for $I_i > 0$ is distinctly smaller than that for $I_i < 0$. This trend is independent of magnetic field, temperature, and wafers. The sensitivity of R'_H to positive/negative polarization is supposed to be nearly symmetric since the measurements are made in a condition with R_H well separated from the upper and lower bounds, $h/(2e^2) < R_H < h/e^2$. We suggest this difference to be attributable to the asymmetric reconstruction of edge channels as discussed by Würtz *et al.*[27,30] With a negative pumping current, $I_i < 0$ ($\Delta\mu > 0$), elastic scattering dominates in the reconstructed edge channels as illustrated in the top panel of Fig. 2(a). With $\Delta\mu < 0$, however, another channel of inelastic interedge-state scattering opens up as schematically illustrated in the lower two panels of Fig. 2(a). In this condition, efficiency of DNP is expected to be significantly smaller since the inelastic scattering may be dominated by spin-orbit interaction, not accompanied by nuclear spin flips.

The fractional ratio of polarized nuclear spins in the experiments can be estimated from the magnitude of resistance change ΔR. We define T as the probability for electrons exiting the source contact to be transmitted to the Hall voltage probe, which is derived from the Hall resistance R_H as $T = (e^2/h)R_H = \frac{1}{2}[1 + \exp(-\ell_{edge}/\ell_{eq})]$,[19] where ℓ_{eq} is the interedge-channel equilibration length. We assume that interedge scattering is dominated by spin-orbit interaction when the resistance is measured with a small alternating current (1 nA). The equilibration length is then calculated from the spinor overlap[17] and found to be dependent on the energy

splitting as $\ell_{eq} \propto B_{eff}^2$, where $B_{eff}=B+\Delta B$ is the total effective magnetic field. Hence the change in the transmission probability ΔT corresponding to the DNP-induced field ΔB is given by

$$\frac{\Delta B}{B} = -\frac{\Delta T}{(2T-1)\ln(2T-1)}.$$

We find $\Delta B/B=-0.26$ or $\Delta B=-1.1$ T for $I_i=-5$ nA and $T_i=120$ s. Noting that $\Delta B_{full}=5.3$ T is achieved when nuclear spins are fully polarized,[31] we find 21% of the nuclear spins are polarized. This estimate is in substantial agreement with a report for a similar device.[32] Efficient pumping and detection of localized nuclear spin polarization prove that this experimental technique is highly promising for quantum mechanical manipulation of nuclear spins in solid-state devices.

IV. DIFFUSION AND RELAXATION

Figure 5(a) displays the profiles of nuclear polarization studied in repeated six scans of V_G after pumping, as schematically shown in the third panel from the top in Fig. 2(b). The condition of pumping is such that $I_i=\pm 5$ nA, $T_i=60$ s, and $X_i=347$ nm. Clearly polarization decays at each scan of 12 s, and a decay time is roughly on the order of 100 s. Different mechanisms are incorporated in the decay process, such as diffusion, electron-nuclear spin flip-flop scattering, and spin-lattice relaxation. The spin-lattice relaxation time in GaAs crystals at low temperature is nearly $T_1 \sim 1000$ s,[33] which is much longer than the decay time found in the data in Fig. 5(a). It is hence evident that diffusion and flip-flop scattering should be relevant. Diffusion to surrounding unpolarized nuclei is expected to play a significant role because the present polarization is confined in a narrow approximately 10-nm-thick layer in the z direction perpendicular to the 2DEG. In order to probe the decay of nuclear polarization, however, it is necessary to have a contact to the edge channels or 2DEG, which inevitably introduces electron-nuclear spin flip-flop scattering. In the measurements of Fig. 5(a), therefore, the effect of diffusion and that of electron-nuclear spin flip-flop scattering cannot be distinguished.

To separate these two effects, we control the contact of nuclear polarization to the 2DEG during the course of decay. For this sake, after pumping nuclear polarization for T_i at $x=X_i$, we wait for a time T_w before scanning the edge channels as schematically shown in the bottom panel of Fig. 2(b). During T_w, we place the edge channels at $x=X_w$, so that nuclear polarization is in contact with the 2DEG only in the region of $x \geq X_w$ during the decay. After the decay for T_w, a "snapshot" of the profile of polarization is taken with a quick scan of 5 s ($X=724$ nm $\rightarrow 124$ nm). Once the procedure in the above is completed, we take 30 min interruption for complete equilibration of the nuclear spin system, and repeat a similar procedure from the beginning by taking a different waiting time T_w.

Each column in Fig. 5(b) displays the profiles obtained after waiting for $T_w=0$, 5, 10, 20, 40, 80, 160, 300, and 600 s, where nuclear polarization is pumped with $I_i=\pm 5$ nA

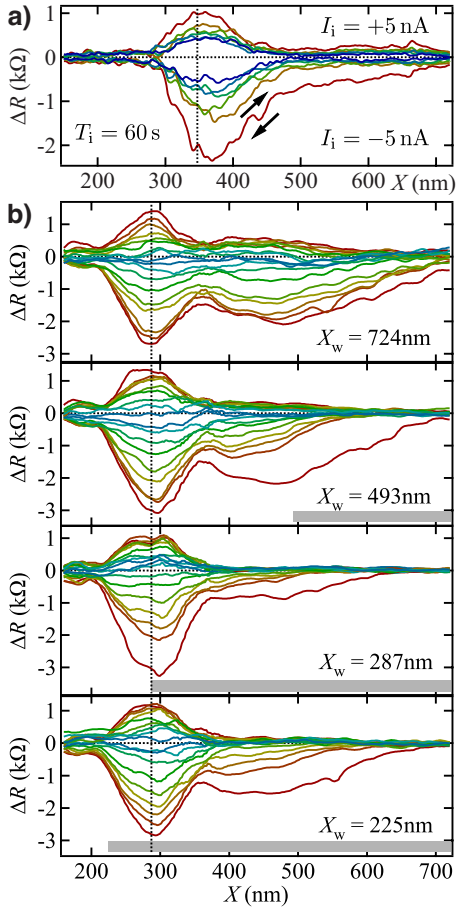

FIG. 5. (Color online) (a) Nuclear polarization, decaying in successive back-and-forth scans of V_G [the sequence in the third panel from the top in Fig. 2(b)]. Pumping is made with $I_i=\pm 5$ nA for $T_i=60$ s at $X_i=347$ nm. (b) Each panel displays the profiles obtained after waiting for a period of $T_w=0$, 5, 10, 20, 40, 80, 160, 300, and 600 s [bottom panel of Fig. 2(b)], where pumping is made with $I_i=\pm 5$ nA for $T_i=60$ s at $X_i=287$ nm. During the waiting time T_w, the edge channels are placed at $X=X_w$ with its value indicated in each panel. All the data here are obtained in single-shot measurements, without averaging different scans.

(Ref. 34) for $T_i=60$ s at $X_i=287$ nm. The four columns correspond to $X_w=724$, 493, 287, and 225 nm from the top. Differently from the measurements for Figs. 1, 3, and 4, each trace is obtained in one sequence of the measurement procedure. The data in Fig. 5(b) shows that, in general, nuclear polarization decays more quickly in the region ($X \geq X_w$) where polarization is in contact with the 2DEG. Closer look at the data shows that the decay rate increases with increasing X in the region of $X \geq X_w$. This behavior, which is ascribed to the collective spin excitation (skyrmion), will be discussed in detail elsewhere. Below we limit our discussion to the region around $X=X_i$.

Figure 6 shows the amplitudes of nuclear polarization ($|\Delta R|$) at $X=X_i=287$ nm as a function of T_w, where the experimental values are taken from the data for $I_i=-5$ nA in Fig. 5(b). The top panel shows the decay occurring when the polarization is isolated from the 2DEG ($X_i < X_w = 493, 724$ nm). The middle panel shows the decay of the polarization placed exactly at the edge of the 2DEG (X_i

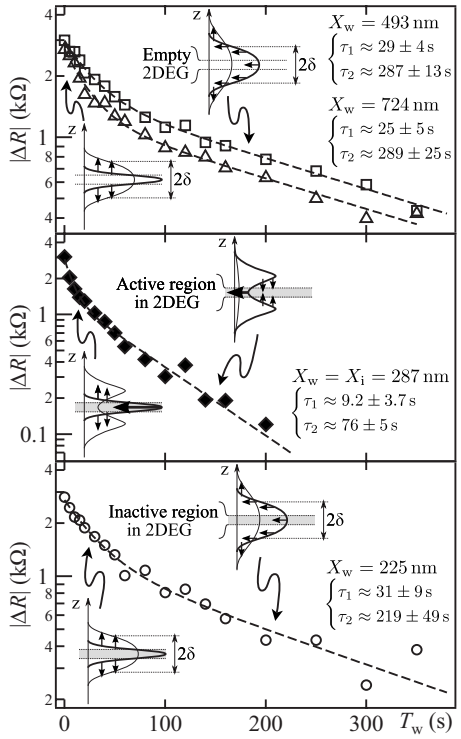

FIG. 6. Semilogarithmic plots of the decay of nuclear polarization at $X=X_i=287$ nm, replotted from the data in Fig. 5(b). Different panels display the data obtained with different relative positions of the polarization and the 2DEG edge, viz., $X_i<X_w$ (top), $X_i=X_w$ (middle), and $X_i>X_w$ (bottom). The dashed lines indicate double-exponential decay curves fitted to the data with the decay times τ_1 and τ_2.

$=X_w=287$ nm) and the bottom panel shows that of the polarization in an interior region of the 2DEG ($X_i>X_w=225$ nm). All the curves in Fig. 6 are well fitted to a double-exponential function, $\Delta R_1 \exp(-T_w/\tau_1)+\Delta R_2 \exp(-T_w/\tau_2)$, as reported by Deviatov *et al.*[30] When the polarization is isolated from the 2DEG (the top panel), it first decays quickly with $\tau_1 \sim 30$ s, followed by a slower decay with $\tau_2 \sim 300$ s. The decay is more rapid when the polarization is in contact with the edge channels (the middle panel), being characterized by $\tau_1=9$ s and $\tau_2=76$ s. When the polarization is placed deeper in the 2DEG ($\nu>1$, the bottom panel), the features of the decay are similar to that when the polarization is isolated from the 2DEG.

Nuclear spin relaxation via the contact hyperfine interaction with the electron spin system is possible in the $\nu=1$ incompressible region but is impossible in the region of $\nu>1$ at low temperatures because it costs a large electronic Zeeman energy, $|g\mu_B B|/k_B=1.2$ K. It follows that the decay of nuclear polarization is free from the interaction with the 2DEG in both cases of $X_i<X_w$ and $X_i>X_w$. Hence the decay in the two conditions should be similar and is accounted for by diffusion and spin-lattice relaxation. The first quick decay ($\tau_1 \sim 30$ s) is suggested to arise from diffusion in the z direction as schematically shown in the lower insets of the top and bottom panel of Fig. 6. The nuclear polarization is pumped in a narrow region of a thickness (~ 10 nm) given by the z-wise extension of the electron wave function of the 2DEG. The diffusion is expected to dominate until the distribution of the polarization expands to a region of the diffusion radius δ, which is roughly estimated to be $\delta=\sqrt{DT_c} \sim 22$ nm, where $D \sim 1000$ Å^2/s is the diffusion constant for arsenic nuclei in GaAs crystals[35] and $T_c \sim 50$ s is the moment at which the decay rate crosses over from τ_1^{-1} to τ_2^{-1} in the present experiments. As the polarization spreads out, the diffusion process slows down because the gradient of the polarization amplitude reduces. Hence the diffusion eventually balances with the spin-lattice relaxation, giving rise to $\tau_2 \sim 300$ s on the order of T_1.

Lateral diffusion in the x direction should be present as well, though apparently not very remarkable. An x-wise broadening of polarization due to lateral diffusion is visible in Fig. 4(c), which closes up the edge of the normalized distributions obtained with $I_i=\pm 5$ nA for $T_i=60$, 300, and 600 s. Extension of the distribution toward smaller X values by ~ 30 nm is discerned during the pumping time of $T_i=600$ s. If a delta-functionlike distribution of nuclear polarization were given instantaneously, the diffusion length of the polarization after $T_i=600$ s would be $\sqrt{DT_i} \sim 80$ nm. In the present experiments, however, nuclear polarization is continuously pumped during T_i, which reduces apparent effect of diffusion. The observed magnitude of broadening (~ 30 nm) on the same order as, but smaller than, 80 nm is therefore consistently attributed to diffusion.

More rapid decay in the condition of $X_i=X_w$ (the middle panel in Fig. 6) is a consequence that electron-nuclear spin flip-flop scattering is possible in the vicinity of the $\nu=1$ incompressible stripe. (This is a counter process to the DNP.) Hence the 2DEG layer serves as a "sink" of the nuclear spin polarization. For detailed interpretation, however, diffusion is to be taken into account as well. The pumped polarization will quickly decay with τ_1 because two channels, the z-wise diffusion and the flip-flop scattering, are open for the decay, as illustrated in the lower left inset. The nuclear polarization generated via diffusion in the upper and the lower adjacent layers is long lived because of the absence of hyperfine interaction. When the polarization in the region of the 2DEG layer decays to a level lower than the polarization outside the 2DEG layer, the polarization outside starts to diffuse back into the 2DEG layer. The decay rate in this condition is $\tau_2 \approx 80$ s, which is determined by the combination of the back diffusion and the flip-flop relaxation inside the layer as schematically shown in the upper right inset.

V. SUMMARY

Spin-split edge channels have been demonstrated to serve as a unique scanning probe to nuclear spin polarization when they are scanned by a biased side gate (V_G). The scan range is typically about 600 nm for $-2.5<V_G<-0.5$ V. The resolution is ~ 14 nm, determined substantially by the extension of the edge-state wave function (magnetic length). Local nuclear polarization is generated by unequally populated spin-split edge channels in different conditions of pumping current I_i and pumping time T_i. The profiles of the induced nuclear polarization are imaged with the probing technique; they prove to be as narrow as 35 nm for small I_i ($|I_i|$

$=0.1$ nA) but broaden significantly with increasing $|I_i|$. Relaxation of the nuclear polarization is studied by probing after letting the polarization decay for a given waiting time T_w (from 0 up to 600 s). The decay process depends significantly on the relative position of the polarization and the edge channels and the electronic structure of the edge channels. The decay processes are interpreted in terms of the combination of the diffusion in the direction normal to the 2DEG layer, the electron-nuclear spin interaction and the spin-lattice relaxation.

ACKNOWLEDGMENTS

This work is supported by a Grant-in-Aid for Scientific Research A (No. 19204031) from the Japan Society for the Promotion of Science (JSPS).

*t-nakajima@thz.c.u-tokyo.ac.jp

[1] J. R. Petta, A. C. Johnson, J. M. Taylor, E. A. Laird, A. Yacoby, M. D. Lukin, C. M. Marcus, M. P. Hanson, and A. C. Gossard, Science **309**, 2180 (2005).
[2] F. H. L. Koppens, C. Buizert, K. J. Tielrooij, I. T. Vink, K. C. Nowack, T. Meunier, L. P. Kouwenhoven, and L. M. K. Vandersypen, Nature (London) **442**, 766 (2006).
[3] A. V. Khaetskii, D. Loss, and L. Glazman, Phys. Rev. Lett. **88**, 186802 (2002).
[4] A. Johnson, J. Petta, J. Taylor, A. Yacoby, M. Lukin, C. Marcus, M. Hanson, and A. Gossard, Nature (London) **435**, 925 (2005).
[5] F. H. L. Koppens, J. A. Folk, J. M. Elzerman, R. Hanson, L. H. W. van Beveren, I. T. Vink, H. P. Tranitz, W. Wegscheider, L. P. Kouwenhoven, and L. M. K. Vandersypen, Science **309**, 1346 (2005).
[6] F. H. L. Koppens, K. C. Nowack, and L. M. K. Vandersypen, Phys. Rev. Lett. **100**, 236802 (2008).
[7] N. Shenvi, R. de Sousa, and K. B. Whaley, Phys. Rev. B **71**, 224411 (2005).
[8] C. Deng and X. Hu, Phys. Rev. B **73**, 241303(R) (2006).
[9] W. Yao, R. B. Liu, and L. J. Sham, Phys. Rev. B **74**, 195301 (2006).
[10] K. Ono and S. Tarucha, Phys. Rev. Lett. **92**, 256803 (2004).
[11] J. M. Taylor, C. M. Marcus, and M. D. Lukin, Phys. Rev. Lett. **90**, 206803 (2003).
[12] B. Kane, Nature (London) **393**, 133 (1998).
[13] K. R. Wald, L. P. Kouwenhoven, P. L. McEuen, N. C. van der Vaart, and C. T. Foxon, Phys. Rev. Lett. **73**, 1011 (1994).
[14] D. C. Dixon, K. R. Wald, P. L. McEuen, and M. R. Melloch, Phys. Rev. B **56**, 4743 (1997).
[15] T. Machida, T. Yamazaki, and S. Komiyama, Appl. Phys. Lett. **80**, 4178 (2002).
[16] A. Würtz, T. Müller, A. Lorke, D. Reuter, and A. D. Wieck, Phys. Rev. Lett. **95**, 056802 (2005).
[17] G. Müller, D. Weiss, A. V. Khaetskii, K. von Klitzing, S. Koch, H. Nickel, W. Schlapp, and R. Lösch, Phys. Rev. B **45**, 3932 (1992).
[18] M. Büttiker, Phys. Rev. Lett. **57**, 1761 (1986).
[19] S. Komiyama and H. Hirai, Phys. Rev. B **40**, 7767 (1989).
[20] G. Müller, D. Weiss, S. Koch, K. von Klitzing, H. Nickel, W. Schlapp, and R. Lösch, Phys. Rev. B **42**, 7633 (1990).
[21] I. A. Larkin and J. H. Davies, Phys. Rev. B **52**, R5535 (1995).
[22] Y. Acremann, T. Heinzel, K. Ensslin, E. Gini, H. Melchior, and M. Holland, Phys. Rev. B **59**, 2116 (1999).
[23] D. B. Chklovskii, B. I. Shklovskii, and L. I. Glazman, Phys. Rev. B **46**, 4026 (1992).
[24] During the pumping for $T_i=60$ s, nuclear polarization diffuses to $\sqrt{DT_i}\sim 24$ nm (see discussion in Sec. IV). However, the profile in the close vicinity of $X\approx X_i$ is rather dominated by the distribution of the directly pumped polarization.
[25] S. Komiyama, H. Hirai, M. Ohsawa, Y. Matsuda, S. Sasa, and T. Fujii, Phys. Rev. B **45**, 11085 (1992).
[26] N. B. Zhitenev, R. J. Haug, K. Eberl, and K. von Klitzing, Europhys. Lett. **28**, 121 (1994).
[27] A. Würtz, R. Wildfeuer, A. Lorke, E. V. Deviatov, and V. T. Dolgopolov, Phys. Rev. B **65**, 075303 (2002).
[28] J. H. Kim, I. D. Vagner, and L. Xing, Phys. Rev. B **49**, 16777 (1994).
[29] This interpretation is supported by additional experiments not described here: at elevated temperatures up to 500 mK, the backgroundlike component of polarization (in a deeper region of $X>X_i+100$ nm) is found to increase its amplitude, whereas the component of polarization around $X\approx X_i$ diminishes. These findings indicate that phonon-assisted processes are relevant to the generation of the backgroundlike polarization.
[30] E. V. Deviatov, A. Würtz, A. Lorke, M. Y. Melnikov, V. T. Dolgopolov, D. Reuter, and A. D. Wieck, Phys. Rev. B **69**, 115330 (2004).
[31] D. Paget, G. Lampel, B. Sapoval, and V. I. Safarov, Phys. Rev. B **15**, 5780 (1977).
[32] S. Masubuchi, K. Hamaya, and T. Machida, Jpn. J. Appl. Phys. **45**, L522 (2006).
[33] J. A. McNeil and W. G. Clark, Phys. Rev. B **13**, 4705 (1976).
[34] It would be straightforward to adopt the smallest current (0.1 nA) for simpler interpretation. We chose, however, $I_i=\pm 5$ nA because (i) generated polarization is large enough to be probed in a single-shot measurement and (ii) a broader distribution of polarization enables observation of the decay process at different positions (X).
[35] D. Paget, Phys. Rev. B **25**, 4444 (1982).